JES Focus Issue on Progress in Molten Salts and Ionic Liquids

Al Film Electrodeposition from the $AlCl_3$-EMIC Electrolyte under a Magnetic Field

Hitomi Takahashi, Hisayoshi Matsushima,[z] and Mikito Ueda[*]

Faculty of Engineering, Hokkaido University, Sapporo, Hokkaido 060-8628, Japan

The surface structure of Al films electrodeposited in a magnetic field was studied in a $AlCl_3$-1ethyl-3methylimidazolium chloride (EMIC) mixture ionic liquid, focusing on the surface morphology and crystal orientation. Current-dependent measurements reveal two preferential orientations. First, at small current densities ($i < 10$ mA cm^{-2}), a (111) plane is preferentially oriented parallel to the surface where no magnetic field is detected. Second, at high current densities ($i > 10$ mA cm^{-2}), a (200) plane is selectively grown, where the mass transportation of Al(III) is promoted by magneto-hydrodynamic (MHD) convection. Correlations of these data with scanning electron microscope observations showing tabular-facet formation in the magnetic field suggest that these structural variations are induced by microscopic MHD, demonstrating the difference between this process and that existing in an aqueous system.

Manuscript submitted February 14, 2017; revised manuscript received March 29, 2017. Published May 9, 2017. *This paper is part of the JES Focus Issue on Progress in Molten Salts and Ionic Liquids.*

Aluminum is a very important material because of its distinctive features of a bright silvery appearance, light weight and high corrosion resistance.[1] Also, because Al exists in abundance it can sustain the current strong demand for building construction and ornamental material. Furthermore, it is used as a base in light-emitting diodes owing to its high reflectance of more than 90% in the visible light region. Several methods such as sputtering,[2,3] vacuum vapor deposition,[4–6] hot dipping[7–10] and electroplating[11–14] have been developed for Al film manufacture.

Dry film manufacturing processes such as sputtering and vapor deposition are mainly employed to produce glossy surfaces, but it is difficult with these processes to coat an intricate substrate or to fabricate a thick film. The hot dipping method can plate sizable objects in large quantities, but precise control of the surface structure is difficult. The electrolytic plating process, however, can overcome these various problems existing in the technical and economical viewpoints, and can lead to new developments in Al film application.

Al electrodeposition is performed in molten salt,[15–17] organic solvents[18,19] and ionic liquid solution.[12,14,20] Room-temperature ionic liquids have attracted much attention because of their ease of operation owing to features such as non-flammability and low vapor pressure. In particular, 1-ethyl-3-methylimidazoliumchloride (EMIC) is well-known as being suitable for Al deposition owing to its high electrical conductivity.[11] Many researchers have investigated Al deposition to produce a shiny surface,[18,21–23] and we have previously carried out Al electrodeposition with additives and reported a shiny coating under the control of a stirred flow.[24] In that work, the surface roughness was drastically improved by increasing the stirring rate, but it was still difficult to form a glossy surface on a complex substrate containing features such as ditches or cavities by the use of mechanical convection alone.

To pursue a novel convection method, we consider that the superimposition of a magnetic field, **B**, is a possible solution. A number of research groups have reported the appearance of unique phenomena when magnetic fields are superimposed on the electrodeposition processes.[25–32] When electrodeposition is conducted in the presence of **B**, for instance, magneto-hydrodynamic (MHD) convection is induced by the electromagnetic interaction. Effect of the magnetic field on the metals electrodeposition from the aqueous electrolytes widely investigated,[25–27,33,34] while the same data for the ionic liquids are very few. We consider, therefore, that fundamental investigation is necessary to clarify the effects of the magnetic field on Al electrodeposition. Thus, the purpose of this research is the investigation of MHD convection influencing on the Al deposition process. Herein, Al films were electrodeposited in EMIC-$AlCl_3$ solution under a uniform magnetic field, whereupon their morphology and crystal orientation were analyzed by scanning electron microscopy (SEM) and X-ray diffractometry (XRD).

Experimental

Electrodeposition was carried out with a three-electrode system, as shown in Fig. 1. The electrolyte used was EMIC(Merck KGaA, Germany)-$AlCl_3$(>98.0 %, Kanto Chemical Co., INC., Japan) ionic liquid, where the molar ratio of EMIC and $AlCl_3$ was 1:2. Ion liquid was prepared under the glove box filled with argon gas because $AlCl_3$ is hygroscopic. After preparing the ionic liquid, aluminum wire was immersed into ionic liquid in order to remove impurities such as moisture by the decomposition reaction. The cathode was a Cu plate ($5 \times 5 \times 0.4$ mm^3, Cu 99.96%, Nilaco Corporation, Japan), and the anode was an Al plate ($10 \times 35 \times 0.5$ mm^3, Al 99.99%, Nippon Light

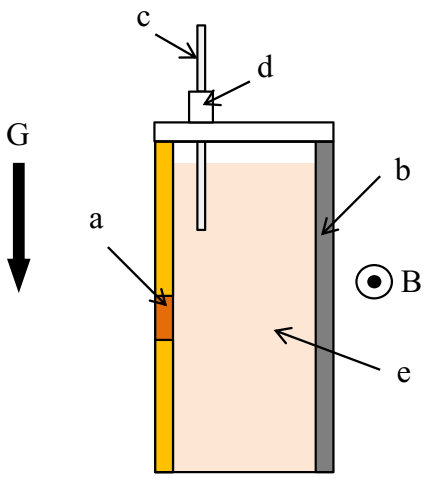

Figure 1. Schematic of the experimental cell showing the cathode (Cu, 25 mm^2) (a), anode (Al, 350 mm^2) (b), reference electrode (Al wire, $\phi = 0.5$ mm) (c), silicon cap (d) and ionic liquid (e). Also shown are the directions of the external magnetic field, **B**, and the force of gravity, *G*.

*Electrochemical Society Member.
[z]E-mail: matsushima@eng.hokudai.ac.jp

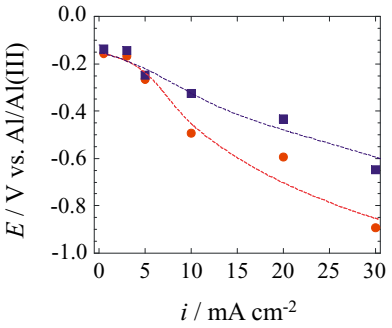

Figure 2. Potential–current plots for Al electrodeposition in EMIC-$AlCl_3$ ionic liquid at 60°C in a magnetic field of 0 T (red ●) and 0.3 T (blue ■).

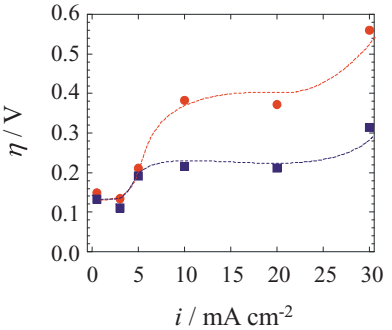

Figure 3. The overpotential, η, as a function of the applied current density, *i*, for Al electrodeposition in EMIC-$AlCl_3$ ionic liquid at 60°C in 0 T (red ●) and 0.3 T (blue ■) magnetic field.

Metal Company, Japan). The electrodes were embedded in either side of the cell walls, facing each other and separated by a distance of 10 mm. Before the experiments, the Cu substrate was polished using abrasive paper and was subsequently dipped (i.e., acid pickling) in a mixture solution of 0.1 mol L^{-1} H_2SO_4 and 0.1 wt% H_2O_2. After acid pickling for 60 s, the substrate was ultrasonically washed, first with pure distilled water and then with acetone for 10 min each. The reference electrode used was an Al wire (0.5 mm diameter, Al 99.99%, Nilaco Corporation, Japan).

All experiments were conducted in a glove box purged using pure Ar gas, where the ionic liquid was kept at 60°C on a hot plate. Al electrodeposition and IR measurement was conducted by potentiostat with frequency analyzer (HZ-5000, Hokuto Denko Corporation, Japan). The electrodeposition was carried out until the amount of electrical charge reached 29 C cm^{-2}, which corresponds to a deposition 10 μm thick. A static and uniform magnetic field of 0.3 T was applied parallel to the electrode surface, where the magnetic field was generated by a permanent magnet (NEOMAX, Sumitomo Special Metals, Japan).

The surface morphology of the electrodeposited Al films was observed using SEM (JSM-6010PLUS/LA, JEOL, Japan), while the crystal orientation was measured by XRD (D2PHASER, Bruker, Germany) using the Cu-Kα line. The resistance of the ionic liquid was obtained by impedance measurement.

Results and Discussion

The Al films were electrodeposited at the varying current densities of 0.5, 3, 5, 10, 20 and 30 mA cm^{-2}, where the deposition time varied from about 16 h to 16 min. The transient behavior of the deposition potential did not exhibit any remarkable difference as a function of the applied current, and the potential value reached its steady state value about 2 min after starting electrolysis. Figure 2 plots the steady state cathode potential, *E*, as a function of current density for Al deposited with and without **B**. It can be seen that the potential change in the low current density values from 0.5 to 3 mA cm^{-2} is a little, whereas it enlarges significantly at current density values greater than 5 mA cm^{-2}. Also, the absolute value of the cathodic potential seems to increase proportionally to the applied current. When the measurement was carried out at 30 mA cm^{-2}, the potential reached −0.9 V in no **B**. Even at high potentials, evolution of the bubble formation on the cathode and a color change of the electrolyte, which indicates decomposition of the ionic liquid, were not detected.

The magnetic field influenced the deposition potential at higher than 5 mA cm^{-2}. It is difficult to discuss the mass transport phenomena because the current was controlled, but we assume that the diffusion of Al(III) does not reach its limitation. This is based on the fact that the diffusion limitation has typically been reported to occur at more than about 50 mA cm^{-2}.[11] Previously, we have reported an aqueous experiment in which Cu was electrodeposited in a high magnetic field of 5 T, and where it was found that the Cu deposition potential was not measurably changed in the non-diffusion control region.[31] Compared with this previous result of the aqueous electrolyte, the present potential exhibits a significant shift toward the noble direction at a low **B** intensity of 0.3 T.

In Fig. 3, the cathode potential was compensated by removing ohmic resistance to clarify the effect of **B** on the deposition overpotential, η. When the electrodeposition was conducted at $i < 5$ mA cm^{-2}, the η was found to be independent of **B**. Presumably, electron transfer was the main factor for this controlling reaction. This result agrees with that of Coey et al.,[35] who reported that **B** had no influence on the activation energy relating to the electron reaction.[31] The overpotential in **B** was reduced by 0.2 V for current densities ranging from 10–20 mA cm^{-2}, wherein the Al(III) reduction reaction gradually became governed by the mass transportation. However, the degree of η reduction at 30 mA cm^{-2} was greater.

The reason for the reduced overpotential in the presence of **B** may be explained by MHD convection. The value of η corresponds to the Al(III) concentration overpotential at high current densities ($i > 10$ mA cm^{-2}), and the present setup was designed for the MHD convection to flow in the same direction as the natural convection. In this way, the string effect could assist the Al(III) diffusion from the bottom to the top of the cathode surface.

The Al films were uniformly deposited on a Cu substrate, and appeared gray in color without any luster. The SEM images show that the crystal grains change remarkably in the presence of a **B** field, where a typical morphological variation is shown in Fig. 4. The SEM image in Fig. 4a shows angular deposits around 1.0 μm in size, and a surface covered with fine irregular grains. The application of **B**, however, created large grains with tabular-facet planes 2–4 μm in size (Fig. 4b), although no additives were used in the present experiments. This suggests that lateral crystal growth is dominant in the ionic liquid as well as in the aqueous system.[26] The nucleation number in the presence of **B** may be suppressed owing to the difference of growth mode.

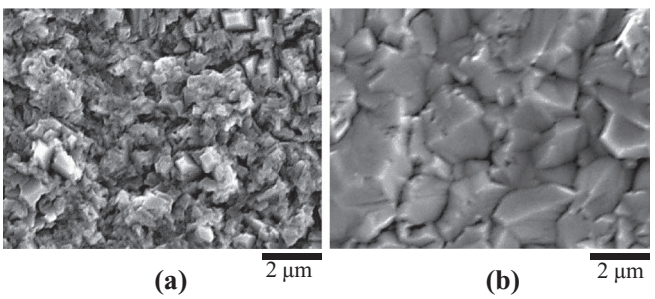

Figure 4. Scanning electron microscope images of Al films electrodeposited galvanostatically for 2 minutes at 30 mA cm^{-2} in a magnetic field of (a) 0 T and (b) 0.3 T (Film thickness: 10 μm).

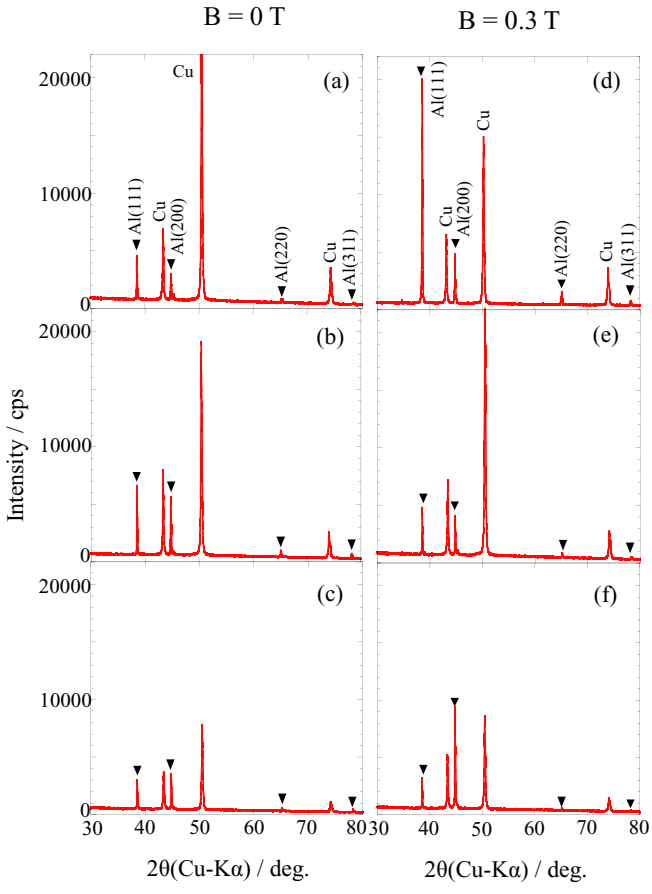

Figure 5. X-ray diffraction spectra of Al films electrodeposited on a Cu substrate at several applied current densities of (a) 5, (b) 10 and (c) 30 mA cm^{-2} in 0 T magnetic field, and (d) 5, (e) 10 and (f) 30 mA cm^{-2} in 0.3 T.

The crystal structure was analyzed by XRD measurement (Fig. 5), wherein aluminum oxide and other impurities were not detected. This again supports the contention that the electrolyte does not deteriorate, as mentioned in Fig. 2. The XRD patterns display four peaks corresponding to the Al crystal structure, where two of them are large peaks attributed to (111) and (200), and the others are small peaks attributed to (220) and (311). The ratio of the diffraction intensity between (111) and (200) was found to depend on the applied current density, where the intensity of (111) decreased with the current, and that of (200) increased with the current. This reversal phenomenon was more pronounced in the presence of a magnetic field.

The orientation index, M, was calculated to quantitatively investigate which crystal orientation is preferentially oriented parallel to the substrate plane. The index M is defined as[36]

$$M = \frac{\frac{I(h\ k\ l)}{\sum I(h'k'l')}}{\frac{I_0(h\ k\ l)}{\sum I_0(h'k'l')}}, \qquad [1]$$

where $I(h\ k\ l)$ is the XRD intensity in the experimental data, $I_0(h\ k\ l)$ is the intensity given in the JCPDS cards (powder pattern). In the present case, $\sum I(h'k'l')$ is the sum of the intensities of the four independent peaks of (111), (200), (220) and (311).

Figure 6 shows the dependency of M on the applied current density in the presence and the absence of **B**, where the preferential orientation is dominated by the (200) and (111) planes. Interestingly the influence of the magnetic field is clearly demonstrated in the ionic liquid electrolyte, although a low **B** intensity of 0.3 T scarcely changes the crystal orientation in aqueous electrolytes.[26] When Al was electrodeposited at a high current density ($i > 10$ mA cm^{-2}), the application of

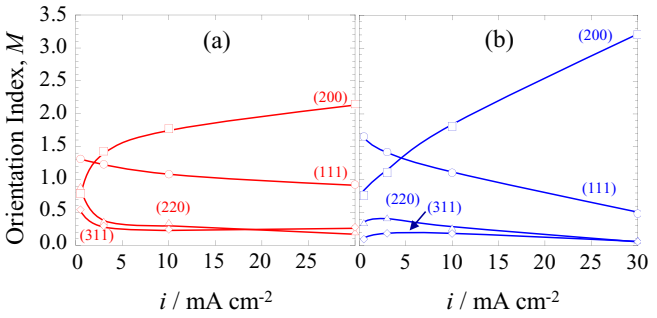

Figure 6. The orientation index, M, as a function of the applied current density, i, for the Al films electrodeposited in (a) 0 and (b) 0.3 T magnetic field, showing the (111) plane (●), (200) plane (■), (220) plane (▲), and (311) plane (♦).

B significantly promoted the growth of (200). The high orientation of (200) may be attributed to the large facet plane, as shown in Fig. 3b.

The dependence of the preferential Al orientation on the overpotential has been investigated theoretically[37] where, with increasing η, the crystal plane of a face-centered cubic metal was found to orient in the (111) plane, followed by the (200) and then the (220) planes. In the face-centered cubic crystal structure, the atomic packing density of (111) is higher than that of (200), and the surface energy required to form (111) is lower than that for (200).[38,39] This density and surface energy ordering is explained by the differences of the bonding energy summation for each crystal plane. The large value of M(200) at 10–30 mA cm^{-2} suggests that the magnetic field promotes the formation of (200), although the η is reduced.

Further, the stirring effect has also been reported by Choudhary et al.,[39] who found that when Al was electrodeposited using a mechanical stirrer, the (200) instead of (111) is preferentially oriented at a current density of 20 mA cm^{-2}. Also, the value of M(200) remarkably decreased with increased stirring speed. However in the present case, the M(200) increased under the magnetic field, which indicates that MHD flow is distinct from mechanical convection.

Thus, the magnetic field can work directly on an ionic liquid, which is a completely polarized molecular liquid, and may induce the microscopic MHD (micro-MHD) in the vicinity of the cathode surface.[40,41] Therefore, several factors such as the mass transportation and surface adsorption of the ionic liquid, which controls the crystal growth, may be affected by the micro-MHD.

Conclusions

The effect of **B** on Al electrodeposition in an EMIC-$AlCl_3$ ionic liquid at 60°C was investigated. The film structure changed significantly in the presence of a small **B** of 0.3 T, which was a result not found in our previous aqueous experiments. The application of **B** caused less deposition overpotential by 0.2 V when Al was electrodeposited at current densities $i \geq 10$ mA cm^{-2}. The orientation index of M(200) was enlarged in **B**, corresponding to the formation of a tabular-faceted surface.

References

1. L. Barchi, U. Bardi, S. Caporali, M. Fantini, A. Scrivani, and A. Scrivani, *Progress in Organic Coatings*, **68**, 120 (2010).
2. G. M. Jellum and D. B. Graves, *Journal of Applied Physics*, **67**, 6490 (1990).
3. C. E. Wickersham Jr., J. E. Poole, A. Leybovich, and L. Zhu, *Journal of Vacuum Science & Technology A*, **19**, 2767 (2001).
4. W. L. Gladfelter, D. C. Boyd, and K. F. Jensen, *Chemistry of Materials*, **1**, 339 (1989).
5. B. E. Bent, R. G. Nuzzo, and L. H. Dubois, *Journal of the American Chemical Society*, **111**, 1634 (1989).
6. S. Guha, E. Cartier, N. A. Bojarczuk, J. Bruley, L. Gignac, and J. Karasinski, *Journal of Applied Physics*, **90**, 512 (2001).
7. L. Lihong, S. Dejiu, Z. Jingwu, S. Jian, and L. Liang, *Applied Surface Science*, **257**, 4144 (2011).
8. W. Deqing, S. Ziyuan, and Z. Longjiang, *Applied Surface Science*, **214**, 304 (2003).
9. F. Barbier, D. Manuelli, and K. Bouché, *Scripta Materialia*, **36**, 425 (1997).

10. E. Serra, H. Glasbrenner, and A. Perujo, *Fusion Engineering and Design*, **41**, 149 (1998).
11. T. Jiang, M. J. C. Brym, G. Dubé, A. Lasia, and G. M. Brisard, *Surface & Coatings Technology*, **201**, 1 (2006).
12. J. K. Chang, S. Y. Chen, W. T. Tsai, M. J. Deng, and I. W. Sun, *Electrochemistry Communications*, **9**, 1602 (2007).
13. B. Li, C. Fan, Y. Chen, J. Lou, and L. Yan, *Electrochimica Acta*, **56**, 5478 (2011).
14. A. P. Abbott, C. A. Eardley, N. R. S. Farley, G. A. Griffith, and A. Pratt, *Journal of Applied Electrochemistry*, **31**, 1345 (2001).
15. W. Simka, D. Puszczyk, and G. Nawrat, *Electrochimica Acta*, **54**, 5307 (2009).
16. M. Jafarian, F. Gobal, I. Danaee, and M. G. Mahjani, *Electrochimica Acta*, **52**, 5437 (2007).
17. M. Jafarian, M. G. Mahjani, F. Gobal, and I. Danaee, *Journal of Applied Electrochemistry*, **36**, 1169 (2006).
18. M. Miyake, Y. Kubo, and T. Hirato, *Electrochimica Acta*, **120**, 423 (2014).
19. Y. Zhao and T. J. V. Noot, *Electrochimica Acta*, **42**, 3 (1997).
20. J. Tang and K. Azumi, *Electrochimica Acta*, **56**, 1130 (2011).
21. S. Z. E. Abedin, P. Giridhar, P. Schwab, and F. Endres, *Electrochemistry Communications*, **12**, 1084 (2010).
22. L. Barchi, U. Bardi, S. Caporali, M. Fantini, A. Scrivani, and A. Scrivani, *Progress in Organic Coatings*, **67**, 146 (2010).
23. K. Uehara, K. Yamazaki, T. Gunji, S. Kaneko, T. Tanabe, T. Ohsaka, and F. Matsumoto, *Electrochimica Acta*, **215**, 556 (2016).
24. H. Takahashi, C. Namekata, T. Kikuchi, H. Matsushima, and M. Ueda, *Journal of the Surface Finishing Society of Japan*, **68**, 208 (2017).
25. A. Bund, S. Koehler, H. H. Kuehnlein, and W. Plieth, *Electrochimica Acta*, **49**, 147 (2003).
26. H. Matsushima, T. Nohira, I. Mogi, and Y. Ito, *Surface and Coatings Technology*, **179**, 245 (2004).
27. A. Krause, M. Uhlemann, A. Gebert, and L. Schultz, *Electrochimica Acta*, **49**, 4127 (2004).
28. C. Wang, Y. B. Zhong, J. Wang, Z. Q. Wang, W. L. Ren, Z. S. Lei, and Z. M. Ren, *Journal of Electroanalytical Chemistry*, **630**, 42 (2009).
29. J. A. Koza, M. Uhlemann, A. Gebert, and L. Schultz, *Journal of Electroanalytical Chemistry*, **617**, 194 (2008).
30. X. Yang, K. Eckert, S. Mühlenhoff, and S. Odenbach, *Electrochimica Acta*, **54**, 7056 (2009).
31. H. Matsushima, A. Bund, W. Plieth, S. Kikuchi, and Y. Fukunaka, *Electrochimica Acta*, **53**, 161 (2007).
32. S. Mohan, G. Saravanan, and A. Bund, *Electrochimica Acta*, **64**, 94 (2012).
33. T. Z. Fahidy, *Progress in Surface Science*, **68**, 155 (2001).
34. O. Devos, A. Olivier, J. P. Chopart, O. Aaboubi, and G. Maurin, *Journal of The Electrochemical Society*, **145**, 401 (1998).
35. F. M. F. Rhen, D. Fernandez, G. Hinds, and J. M. D. Coey, *Journal of The Electrochemical Society*, **153**, J1 (2006).
36. S. Yoshimura, S. Yoshihara, T. Shirakashi, and E. Sato, *Electrochimica Acta*, **39**, 589 (1994).
37. N. A. Pangarov, *Journal of Electroanalytical Chemistry*, **9**, 70 (1965).
38. J. P. Zhao, X. Wang, Z. Y. Chen, S. Q. Yang, T. S. Shi, and X. H. Liu, *Journal of Physics. D*, **30**, 5 (1997).
39. R. K. Choudhary, V. Kain, and R. C. Hubli, *Surface Engineering*, **30**, 562 (2014).
40. R. Aogaki, R. Morimoto, and M. Asanuma, *Journal of Magnetism and Magnetic Materials*, **322**, 1664 (2010).
41. H. Matsushima, T. Nohira, and Y. Ito, *Electrochemical and Solid-State Letters*, **7**, C81 (2004).